Transforming Growth Factor Beta 1 drives a switch in connexin mediated cell-to-cell communication in tubular cells of the diabetic kidney

*Hills CE[1], *Price GW[1], Wall MJ[2], Kauffman TJ[2], Tang SC[3], Yiu WH[3], Squires PE[1]

1. Joseph Banks Laboratories, Green Lane, University of Lincoln, Lincoln, UK
2. School of Life Sciences, Gibbet Hill, University of Warwick, Warwick, UK
3. Division of Nephrology, Department of Medicine, The University of Hong Kong, Queen Mary Hospital, Hong Kong, China

*Joint 1st author

Corresponding author

Dr Claire Hills
Joseph Banks Laboratories
University of Lincoln
Lincoln
LN6 7DL
chills@lincoln.ac.uk
01522 886918

Abstract

Aims/Hypothesis: Changes in cell-to-cell communication have been linked to several secondary complications of diabetes, but the mechanism by which connexins affect disease progression in the kidney is poorly understood. This study examines a role for glucose-evoked changes in the beta1 isoform of transforming growth factor (TGFβ1), on connexin expression, gap-junction mediated intercellular communication (GJIC) and hemi-channel ATP release from tubular epithelial cells of the proximal renal nephron.

Methods: Biopsy material from patients with and without diabetic nephropathy was stained for connexin-26 (CX26) and connexin-43 (CX43). Changes in expression were corroborated by immunoblot analysis in human primary proximal tubule epithelial cells (hPTECs) and model epithelial cells from human renal proximal tubules (HK2) cultured in either low glucose (5mmol/L) ± TGFβ1 (2-10ng/ml) or high glucose (25mmol/L) for 48h or 7days. Secretion of the cytokine was determined by ELISA. Paired whole cell patch clamp recordings were used to measure junctional conductance in control versus TGFβ1 treated (10ng/ml) HK2 cells, with carboxyfluorescein uptake and ATP-biosensing assessing hemi-channel function. A downstream role for ATP in mediating the effects of TGF-β1 on connexin mediated cell communication was assessed by incubating cells with ATPγS (1-100μM) or TGF-β1 +/- apyrase (5 Units/ml). Implications of ATP release were measured through immunoblot analysis of interleukin 6 (IL-6) and fibronectin expression.

Results: Biopsy material from patients with diabetic nephropathy exhibited increased tubular expression of CX26 and CX43 ($P<0.01$, n=10), data corroborated in HK2 and hPTEC cells cultured in TGFβ1 (10ng/ml) for 7days ($P<0.001$, n=3). High glucose significantly increased TGFβ1 secretion from tubular epithelial cells ($P<0.001$, n=3). The cytokine (10ng/ml) reduced junctional conductance between HK2 cells from 4.5±1.3nS in control to 1.15±0.9nS following 48h TGFβ1 and to 0.42±0.2nS after 7days TGFβ1 incubation ($P<0.05$, n=5). Acute (48h) and chronic (7day) challenge with TGFβ1 produced a carbenoxolone (200μM)-sensitive increase in carboxyfluorescein loading, matched by an increase in ATP release from 0.29±0.06μM in control to 1.99±0.47μM after 48hr incubation with TGFβ1 (10ng/ml; $P<0.05$, n=3). TGF-β1 (2-10ng/ml) and ATPγs (1-100μM) increased expression of IL-6 ($P<0.001$ n=3) and fibronectin ($P<0.01$ n=3). The effect of TGF-β1 on IL-6 and fibronectin expression was partially blunted when preincubated with apyrase (n=3).

Conclusion: These data suggest that chronic exposure to glucose-evoked TGFβ1 induce an increase in CX26 and CX43 expression, consistent with changes observed in tubular epithelia from patients with diabetic nephropathy. Despite increased connexin expression, direct GJIC communication decreases, whilst hemichannel expression/function and paracrine release of ATP increases, changes that trigger increased levels of expression of interleukin 6 and fibronectin. Linked to inflammation and fibrosis, local increases in purinergic signals may exacerbate disease

progression and highlight connexin mediated cell communication as a future therapeutic target for diabetic nephropathy

Keywords: diabetic nephropathy, tubular epithelia, TGFβ, connexin, bio-sensing, hemi-channels, gap-junctions, ATP, inflammation, fibrosis.

Introduction

Diabetic nephropathy (DN) is the single commonest cause of entry into the renal replacement programme, and with the incidence of the disease doubling in the past decade, it now accounts for approximately 50% of patients presenting with end-stage renal failure [1]. Associated with both inflammation and fibrosis [2-3], understanding the mechanism by which glucose evoked changes in TGF-β instigate these phenotypic and morphological changes in the kidney, is essential in establishing novel therapeutic strategies for the arrest and/or prevention of the disease.

In diabetic nephropathy, for cells to function efficiently and adapt appropriately in times of stress, they must not only interact with each other, but also with their immediate environment. Cells communicate with their neighbours via direct gap junction intercellular communication or through hemichannel mediated paracrine signalling [4-5]. Cells utilise a class of membrane bound proteins called connexins (CX), which cluster into a hexameric structure enabling formation of a trans-membrane pore more commonly termed a connexon [6]. These connexons, alternatively known as hemi-channels; align with those on adjacent cells and 'dock' to form a gap junction. This junction facilitates the transmission of metabolic and electrical signals directly between cells, enabling cells to entrain their activity and synchronise tissue function. In the absence of neighbouring partners, uncoupled hemi-channels permit local paracrine release of nucleotides, including adenosine triphosphate (ATP) and its metabolites (ADP, AMP and adenosine) [4][6].

Regulation of connexin synthesis and activity is critical to cell function and a number of diseases can be attributed to changes in expression/function of these important proteins including ischemia [7], inflammation [8] and both renin induced and essential hypertension [9-10]. In diabetes, hyperglycaemia and subsequent altered connexin expression has proved critical in the development and progression of secondary micro-vascular complications, with glucose decreasing gap-junction conductance and disrupting cellular homeostasis in a variety of cell types [11-15]. Glucose-evoked changes in gap-junction conductance and hemi-channel activity have been linked to the pathology of multiple micro-vascular complications of diabetes [12-19], and there is now considerable evidence to suggest that connexins represent a potential therapeutic target in the treatment of secondary complications of the disease [20-21]. Evidence that connexin expression is linked to renal damage [20-22], has led to suggestions that both hemi-channels and gap junctions may represent future therapeutic targets for the treatment of diabetic nephropathy (DN).

Of the 21 known mammalian connexins, nine isoforms are expressed within the human kidney [reviewed in 23]. Whilst studies on renal vasculature have attributed a role for connexins in the regulation of blood pressure [9-10], we still lack a basic understanding of the effects of connexin

mediated cell communication in the tubular epithelia. Furthermore, we know nothing as to how connexin mediated cell communication may contribute to the pathology of the diabetic kidney.

Tubulointerstitial fibrosis represents the key underlying pathology of diabetic nephropathy with progression linked to loss of renal function and entry into End Stage Renal Failure [2]. A consequence of multiple morphological and phenotypic changes, the glucose-dependent beta-1 isoform of the pro-fibrotic cytokine Transforming Growth Factor (TGF-β1) has been demonstrated to be instrumental to this series of events [24]. In the current study we present histological evidence that demonstrates for the first time, that the expression of key isoforms CX26 and CX43 are markedly upregulated in biopsy material obtained from patients with DN. We investigate the effects of glucose-evoked changes in profibrotic TGF-β1 on expression of predominant tubular connexin isoforms 26 and 43 and the implications that these changes have for cell-to-cell communication and subsequent downstream phenotypic changes in human proximal tubule cells. Understanding the contribution of tubular connexin-mediated cell-to-cell communication in the pathogenesis of diabetic nephropathy will help identify potential intervention routes for future treatment.

Methods

Materials

Human primary proximal tubule epithelial cells (hPTECs) and human derived proximal tubule kidney (HK2) epithelial cells were both obtained from ATCC. Tissue culture supplies were purchased from Invitrogen (Paisley, UK). Immobilon P membrane was from Millipore (Watford, UK) and enhanced chemoluminescence from Amersham Biosciences (Amersham, UK). Antibodies Smad2 and Smad3 are monoclonal antibodies that were obtained from Cell signaling Technology (Danvers, MA, USA). Small interfering RNA (siRNA) was obtained from Santa Cruz (Santa Cruz, CA, USA). For western blot analysis, CX26 and IL6 antibodies were obtained from Abcam (Cambridge, UK) and fibronectin from R&D Systems (Abingdon, UK), whilst CX43 antibody was obtained from Santa Cruz . For immunohistochemistry anti-CX26 was obtained from (Santa Cruz, CA, USA) and anti-CX43 (Sigma-Aldrich,MO, USA). Recombinant human TGF-β1, glucose, apyrase and lipofectamine were obtained from Sigma (Poole, UK), as were all other general chemicals. The anti-TGF-β1 ELISA was from R&D Systems. ATP biosensors were from Sarissa Biomedical Ltd (UK) and fluorodishes from WPI (Hertfordshire, UK).

Staining of tissue

Renal biopsies from patients with biopsy-proven diabetic nephropathy (DN) (mean age 55; mean DM duration: 6.2yrs; mean HbA1C: 7.2%; mean serum creatinine: 464 µmol/L; mean proteinuria: 5.80 g/24h) were selected for this study. Normal portions of renal tissues removed from 5 nephrectomy specimens for the treatment of renal carcinoma (mean age 61; mean serum creatinine: 87.8 µmol/L) were used as control. For immunohistochemistry, we included 2 types of samples that were obtained from renal biopsy of diabetic patients with DN (disease group, n=10), and from the normal portion of nephrectomized specimen removed from patients with renal carcinoma (control group, n=6). The staining protocol is described previously [25]. Briefly, paraffin-embedded renal sections (4um) were de-paraffinized, rehydrated and subjected to microwave-based antigen retrieval in 10mM citric buffer solution, followed by quenching in 1% hydrogen peroxide solution and blocking in 2% BSA solution. Each section was stained overnight with either anti-CX26 (Santa Cruz Biotechnology, San Cruz, CA) 1:50 or anti-CX43 (Sigma-Aldrich, St. Louis, MO) 1:100, antibodies and subsequently incubated with DAKO EnVision⁺ System-HRP labeled polymer antibodies (Dako, Carpinteria, CA). Rabbit IgG was incubated with both DN and control renal section as isotype-matched negative control. The immuno-complex was visualized using DAB substrate and counterstained with hematoxylin. Quantitative analysis was measured by Image-Pro Plus 6.0 and presented as a value of integrated optical density (IOD).

Tissue culture

Model cell line

Human kidney (HK2) cells are a proximal tubular cell (PTC) line derived from normal kidney. The cells are immortalized by transduction with human papilloma virus 16 (HPV-16) E6/E7 genes and are mycoplasma free. Human kidney (HK2) cells (passage 18-30) were maintained in DMEM/Hams F12 medium, supplemented with 10% FCS wt/vol, glutamine (2mmol/l) and EGF (5ng/ml), and cultured at 37°C in a humidified atmosphere with 5% CO_2. Prior to treatment, cells were transferred to DMEM/F12 low glucose (5mmol/l) for 48h as described previously [26]. Cells were serum-starved overnight before incubating in TGF-β1 (2–10ng/ml), glucose (25mmol/l), conditioned media or L-glucose (25mmol/l) for 48h. To determine a role for glucose-evoked changes in TGF-β1 over chronic incubation periods, cells were treated with TGF-β1 (10ng/ml) for 7days. For ATP experiments cells were incubated in non-hydrolysable ATPγS (1-100μM) for 48h or 7days with or without the ATP diphosphohydrolase apyrase (5 Units/ml)

Human proximal tubule epithelial cells

Primary human proximal tubule epithelial cells (hPTECs) were maintained in a renal epithelial cell basal medium obtained from ATCC, supplemented with 0.5% FCS wt/vol, Triiodothyronine (10nM), rh EGF (10ng/ml), Hydrocortisone Hemisuccinate (100ng/ml), rh Insulin (5μg/ml), Epinephrine (1μM), Transferrin (5μg/ml), L-Alanyl-L-Glutamine (2.4mM). Cells were cultured at 37°C in a humidified atmosphere with 5% CO_2. Prior to treatment, cells were serum-starved overnight before incubating in TGF-β1 (10ng/ml) for 7days.

Cytoskeletal staining of HK2 cells

At 80% confluence, cells were fixed with 4% paraformaldehyde. After blocking, the nuclear stain DAPI (1mmol/l) was added for 3min. Cells were then incubated for 1h at 25°C with tetramethyl rhodamine isothiocyanate (TRITC)-conjugated phalloidin, diluted at 1:100, in PBS-Triton. Cells were visualized using a fluorescence microscope (Axiovert 200; Carl Zeiss, Welwyn Garden City, UK).

Quantification of TGF-β1

Fraser et al [27-28] previously reported that exposure of HK2 cells to high glucose triggers increased secretion of TGF-β1. Secretion of the cytokine in our model system was confirmed ahead of experiments where cells were incubated in conditioned media. HK2 cells were cultured in 5mmol/l glucose containing media for 48h prior to overnight serum starvation. Cells were stimulated for 7days

with glucose (25mmol/l) under serum-free conditions and total TGF-β1 measured by specific enzyme-linked immunosorbent assay (ELISA) of cell culture supernatant collected from growth-arrested HK2 cells. Active TGF-β1 is measured directly and latent TGF-β1 measured following acid activation of samples. This assay has <1% cross-reactivity for TGF-β2 and TGF-β3. TGF-β1 concentration was normalized to mg/ml of protein. Data were obtained as pico-grams of TGF-β1 per milliliter per mg of protein.

Immunoblotting

Cytosolic proteins were prepared and separated by gel electrophoresis and electro-blotting on to Immobilon P membranes as described previously [29]. Membranes were probed with specific polyclonal antibodies against anti-CX43 and anti-CX26 at dilutions of 1:200 and 1:400 respectively. For assessment of Smad activity, membranes were probed with anti-pSmad2 and anti-pSmad3 at dilutions of 1:1000. For assessment of IL-6 and Fibronectin, membranes were probed with antibodies at dilutions of (1:1000) and (1:1000) respectively.

Smad 2 and Smad 3 SiRNA knockdown

Cells were grown to 40% confluence in six-well plates. Transfection of siRNAs was carried out using lipofectamine as described previously [30]. To confirm a role for Smad2/3 in mediating the downstream effects of TGF-β1 on CX26 and CX43 expression, HK2 cells were stimulated with TGF-β1 (10ng/ml) for 48h post Smad2/3 knockdown. Negative controls included non-transfected cells, lipid alone, and scrambled siRNA. Smad2 and Smad3 knockdown were confirmed by Western blot analysis.

Electrophysiology

Described previously [31], cells cultured on glass cover-slips were transferred to the recording bath and perfused (2ml/min) with physiological saline solution composed of (mM): 127 NaCl, 1.9 KCl, 1.2 KH_2PO_4, 26 $NaHCO_3$, 1 $MgCl_2$, 2$CaCl_2$ and 10 D-Glucose bubbled with 95% O_2/ 5 % CO_2 and maintained at 32□C. Cells were visualized (x600 magnification) using IR-DIC optics (Olympus BX51W1 microscope and Hitachi CCD camera). Paired whole cell patch-clamp recordings were made from neighboring cells using thick-walled borosilicate (Harvard) glass pipettes (3-8MΩ) containing (mM): 135 potassium gluconate, 7 NaCl, 10 HEPES, 0.5 EGTA, 10 phosphocreatine, 2 MgATP, 0.3 NaGTP (∼300 mOSM, pH7.2). Recordings were made using an Axon Multiclamp 700B amplifier (Molecular Devices) and digitized at 20 kHz (Axon Digidata 1440a). Data acquisition and analysis was performed using pClamp (v10, Axon, Molecular Devices).

Once paired whole cell recordings were established, series resistance (10-16MΩ) was monitored and compensated appropriately. If the series resistance markedly changed during the recording, then the data was excluded from analysis. Electrical coupling between recorded cells was

confirmed by observing a change in membrane potential in one cell following injection of hyperpolarizing and depolarizing current steps in the other cell. At the end of recordings, the electrodes were lifted off the cells and identical current steps were injected to ensure that there was no cross talk between electrodes.

Measuring junctional conductance

Input resistance and coupling coefficients (ratio of membrane potential changes between the two cells) were determined from membrane potential responses following the injection of a series of hyperpolarizing and depolarizing current steps into each cell. The junctional conductance (Gj) was then calculated using the following equation: Gj12 = R1k12/((R1R2)-(R1k12)2), where R1 and R2 are the input resistances of the 2 cells and k12 is the coupling coefficient [28-29]. Estimates for junctional conductance were calculated in both directions between pairs of cells.

Carboxyfluorescein loading

Fluorodishes were plated with HK2 cells in DMEM/F12 low glucose (5mmol/l) for 48h. Cells were serum starved overnight before culturing +/- TGF-β1 (10ng/ml) for 48h or 7days. Cells were exposed to a Ca^{2+}-free BSS (zero $CaCl_2$ + EGTA (1mM)), plus carboxyfluorescein (200 µM) for 10 min, followed by a 10 min period in Ca^{2+}-containing BSS, plus carboxyfluorescein (200 µM). The dishes were then washed with control Ca^{2+}-containing BSS to remove excess dye. In a separate series of experiments, cells were pre-incubated with carbenoxolone in Ca^{2+}-free BSS for 30min and carbenoxolone was applied throughout the loading protocol described above. Cells were imaged using a Cool Snap HQ CCD camera (Roper Scientific) with Metamorph image software (Universal Imaging Corp., Marlow, Bucks, UK). Quantification of dye loading was performed using ImageJ. A region of interest (ROI) was drawn around individual cells (15 in each dish) and mean pixel intensity calculated. All values have been corrected for background fluorescence in a representative ROI.

ATP biosensor measurements

Biosensors consist of enzymes trapped within a matrix around a Pt or Pt/Ir (90/10) wire [32] Biosensors were cylindrical with an exposed length of ~2 mm and diameter of ~ 50 µm. Two types of sensor were used in this study: Firstly, null sensors, possessing the matrix but no enzymes, to control for non-specific electro-active interferents and ATP biosensors which consist of the entrapped enzymes glycerol kinase and glycerol-3-phosphate oxidase [33]. Glycerol (2 mM) was included in all solutions as a co-substrate for ATP detection. HK2 cells were grown on coverslips in DMEM/F12 low glucose (5mmol/L) for 48h. Cells were serum-starved overnight before culturing +/- TGF-β1 (10ng/ml) for 48h or 7days. Cells were then transferred to a chamber containing balanced salt solution (BSS) composed of (mM): (137 NaCl, 5.4 KCl, 0.8 $MgSO_4$, 0.3 Na_2HPO_4,

0.4 KH_2PO_4, 4.2 $NaHCO_3$, 10 HEPES and 5 glucose, pH7.4), with $CaCl_2$ (1.3mM) perfused at a rate of 6ml/min (37°C) for 10 min to acclimatise. Before ATP measurements were made, cells were pre-loaded with ATP to increase the signal [34]. Hemi-channels were opened with a 5 min perfusion of Ca^{2+}-free BSS (+ EGTA (1mM)), cells were then incubated with 10 mM ATP in Ca^{2+}-free BSS for 10 mins before the hemi-channels were closed by the addition of Ca^{2+}-containing BSS. Following ATP loading, ATP and null bio-sensors were bent so that the surface of the sensor was parallel to the coverslip, and placed just above the cells. After a stable baseline was established, Ca^{2+}-free BSS was perfused over the cells to open the hemi-channels and release ATP. A standard solution containing ATP (10µM) was used to calibrate against a standard curve and ensure biosensor sensitivity. Recordings were acquired at 1 kHz with a Micro CED (Mark2) interface using Spike (Vs.6.1) software.

Analysis

Autoradiographs were semi-quantified by densitometry (TotalLab 2003; NonLinear Dynamics, Durham, NC USA). Non-stimulated, low-glucose control was normalized to 100% and data from all other experiments compared to this. Statistical analysis was performed using a one-way ANOVA test with Tukey's multiple comparison post-test or a t-test. Data are expressed as mean±SEM, with 'n' denoting the sample number. A *p*-value <0.05 signified statistical significance.

Results

Connexin expression is up-regulated in tubular epithelia from patients with diabetic nephropathy

Glucose-evoked changes in both gap-junction conductance and hemi-channel activity have been linked to the development and progression of multiple micro-vascular complications of diabetes [14-19]. However, despite being highly expressed in the proximal tubule [23], our knowledge of connexin expression in the diabetic kidney is severely limited. Using integrated optical density (IOD) readings to quantify immunohistochemical staining we evaluated expression of the connexin isoforms CX26 (Fig 1a and b) and CX43 (Fig 1c and d) in renal biopsies from patients with and without DN. In non-disease control, CX26 was predominantly expressed in renal tubules, with relatively weak staining in the glomeruli (Fig 1a panels C and D). In biopsy material from patients with DN (Fig 1a panels A and B), tubular expression of CX26 expression was up regulated to 102700±6226 compared to control 21030±4727 (Fig 1 b; n=10 p<0.01). Similarly, tubular expression of CX43 was significantly increased in patients with DN (Fig 1c panels A and B) to 116300±5908, compared to non-diseased control (Fig 1c panels C and D) at 21460±10920 (Fig 1 d; n=10 p<0.01). Rabbit IgG was incubated with both DN and control renal section as an isotype matched negative control (Fig 1e)

Glucose stimulates increased TGF-β1 in human proximal tubule cells

In diabetes, hyperglycaemia instigates multiple downstream signalling pathways, responsible for both inflammation and the accumulation of fibrotic material in the tubulointersitium [2-3]. Whilst more than a dozen fibrogenic factors affect renal function, it is widely recognised that glucose-evoked changes in pro-sclerotic cytokine TGF-β1 and its downstream Smad signalling cascade, represents the predominant pathway in orchestrating renal fibrosis [35]. ELISA on supernatant fractions from glucose treated HK2 cells confirmed glucose-evoked changes in TGF-β1 in cells of the human proximal tubule (Fig 2a) [36]. Cells were cultured in 5mM glucose for 48h prior to being starved of serum overnight and stimulated for 7days with low (5mmol/l) or high D-glucose (25mmol/l) under serum-free conditions. In high glucose, total TGF-β1 secretion increased (994.4±43.6 pg/ml) compared to the 5mmol/l low glucose control (334±14.9 pg/ml; n = 3; p<0.01) (Fig 2a). Differences in TGF-β1 were only detected following acidification of the samples, suggesting that TGF-β1 was produced in its latent form. L-glucose (25mmol/l) failed to increase TGF-β1 secretion and was used as an osmotic control (OC; Fig 2a).

Non-stimulated HK2 cells exhibit a cobblestone morphology characteristic of proximal tubular epithelial cells (Fig 2, panel b, control). Following activation of latent TGF-β1 by repeat freeze-thaw cycles of 7day conditioned (25mmol/l) media [26], 48h treatment of cells with this media altered

gross morphology in favor of an elongated fibrous phenotype, comparable to that observed with TGF-β1 (10ng/ml; Fig 2 panel b). Morphological changes at 48h were accompanied by actin reorganization, with F-actin filaments forming dense peripheral stress fibers in conditioned media and TGF-β1, compared to the diffuse trans-cellular network of actin that spans the cytosol under control conditions (Fig 2 Panel c). Exposure to 25mmol/l D-glucose alone, failed to alter either cell morphology or cytoskeletal architecture (Fig 2 Panels b and c respectively).

Glucose-evoked TGF-β1 has a bi-phasic effect on CX26 and CX43 at 48h and 7days in human proximal tubule cells.

HK2 cells were cultured in 5mM glucose for 48h prior to being serum starved overnight and then incubated for 48h in conditioned media (25mmol/l D-glucose), high D-glucose (25mmol/l), TGF-β1 (2-10ng/ml), or an osmotic control (L-glucose 25mmol/l). Activated conditioned media significantly reduced CX26 (Fig 3a) and CX43 (Fig 3b) expression to 44.3±2.6% and 53.3±2.0% of control (5mmol/l) (n=3; $p<0.001$). D-glucose alone (25mmol/l) failed to alter CX26 expression, however induced a small significant change in CX43 expression. Immunoblot analysis confirmed that 48h incubation with TGF-β1 (2-10 ng/ml) decreased CX26 expression to 72.7±13.3%, 71.6±4.8%, and 58.3±5.7% at 2, 4 and 10ng/ml compared to control (Fig3c; $p<0.001$, n=4), whilst CX43 levels decreased to 61.2±10.4%, 49.5±6.1%, and 48.1±3.8% compared to control (Fig3d; $p<0.001$, n=4).

In contrast, chronic incubation of both HK2 and human primary proximal tubule cells (hPTECS) with TGF-β1 (10ng/ml) for 7days (Fig 4) matched elevated expression in biopsy material isolated from patients with nephropathy (Fig 1). At 7days, non-stimulated hPTEC cells exhibit a cobblestone morphology characteristic of proximal tubular epithelial cells (Fig 4a, panel A, control). Incubation of hPTECS for 7days with TGF-β1 altered gross morphology towards that of an elongated fibrous phenotype (10ng/ml; Fig 4a panel B). Immunoblot analysis confirmed that chronic incubation with TGF-β1 (10ng/ml) for 7days significantly increased the expression of CX26 and CX43 to 203.9±7.5% (Fig4b) and 151.1±7.1% (Fig4c) of control respectively ($p<0.001$, n=4) in HK2 cells. Chronic incubation of hPTECs with TGF-β1 (10ng/ml) for 7days significantly increased the expression of CX26 and CX43 to 309±39% (Fig4d) and 303±10.4% (Fig4e) of control ($p<0.001$, n=4).

TGF-β1 regulates CX26 and CX43 expression via a classical SMAD2/SMAD3 pathway in HK2 cells

TGF-β1 and its downstream Smad and non-Smad signalling mediators, represent the main pathway orchestrating fibrosis in the diabetic kidney [reviewed in 35]. However, it is not clear as to how TGF-β1 mediates its effects on CX26 and CX43. To determine a classic; canonical (Smad signalling) role for glucose evoked changes in TGF-β1 (Fig2a) in regulating CX expression, SMAD

signalling in HK2 cells was confirmed prior to investigating a role for SMAD2/3 in mediating the effects of TGF-β1 on expression of CX26 and CX43.

HK2 cells were cultured in 5mmol/l glucose for 48h prior to overnight serum starvation. Cells were then stimulated between 5min and 6h with TGF-β1 (10ng/ml) and Smad activity assessed via immunoblotting (Fig5). Data confirmed that TGF-β1 optimally phosphorylates Smad2 (Fig 5a) and Smad3 (Fig 5b) at 1h. Prior to delineating the role for Smad2/3 in TGF-β1 evoked changes in connexin expression, transient transfection of HK2 cells with Smad2 and Smad3 siRNA was performed at 48h and 96h to assess knockdown efficiency. At 48h, knockdown of Smad2 (Fig 5c) and Smad3 (Fig 5e) achieved 59.2±2.9% and 70.1±7.2% efficiency compared to control ($p<0.001$, n=3). At 96h, transfection efficiency was 62.9±7.3% for Smad2 (Fig 5d) and 59.8±11.2% for Smad3 (Fig 5f) compared to control ($p<0.001$, n=3). Scrambled siRNA and transfection reagent alone had no effect.

In HK2 cells, TGF-β1 (10ng/ml, 48h) reduced CX26 and CX43 expression to 75.7±3.4% and 66.7±5.5% of control (Fig 5g and h). To determine if this loss in expression was Smad-dependent, cells were transiently transfected with either Smad2 or Smad3 siRNA for 48h, prior to treatment with TGF-β1 (10ng/ml). TGF-β1 induced loss in expression was negated post Smad2/Smad3 knockdown, restoring CX26 expression to 87.5±4.7% and 113.6±5.4% (Fig 5 g) respectively, as compared to TGF-β1 treatment alone (24.34±3.4%). Similarly, Smad2 and Smad3 knockdown restored CX43 expression to 100.6±11.7% and 129±51.5 % respectively (Fig 5h), compared to 48h TGF-β1 treatment alone (33.3±5.5%) ($p<0.001$, n=3).

TGF-β1 evokes an acute and chronic reduction in junctional conductance.
To assess the functional consequence of altered connexin expression, we used paired whole cell patch clamp recordings to measure the junctional conductance between TGF-β1 treated HK2 cells (Fig 6a). Cells were cultured overnight in 5 mmol/l glucose without serum. Cells were then stimulated for 48 h or 7 days with TGF-β1 (10ng/ml) under serum-free conditions and gap junction intercellular communication (GJIC) assessed against non-stimulated control cells. In control, the junctional conductance was 4.5 ± 1.3nS (n = 5, Fig 6b). TGF-β1 significantly decreased junctional conductance at both 48h (1.15 ± 0.9nS; $p<0.05$, n = 5) and 7days (0.42 ± 0.2nS; $p<0.05$, n=5).

TGF-β1 increases hemi-channel activity in HK2 cells
Hemi-channels can be opened experimentally by removing extracellular calcium. When open, uptake of the membrane impermeant dye carboxyfluorescein, acts as a functional measure of hemi-channel number/activity [34]. Following 48h in low (5mmol/l) glucose, HK2 cells were serum starved overnight before a further 48h (Fig 7a and b) or 7day period (Fig 7c and d) +/- TGF-β1

(10ng/ml) under serum-free conditions. After 48h in TGF-β1, removing extracellular calcium (10min) significantly increased carboxyfluorescein (200µM) uptake compared to control (378 ± 33% p<0.001, n=3; 15 cells per dish; Fig 7a/b,). The increase was negated by pre-incubation with the hemi-channel blocker carbenoxolone (200µM; 110 ± 5.4% of control). At 7 days, dye uptake increased to 430 ± 18% compared to control (Fig 7c/d). Pre-incubation with carbenoxolone (200µM) significantly reduced dye uptake in both control and TGF-β1 treated cells to 41±2.7% and 64±2.6% respectively (p<0.001, n=3).

TGF-β1 increases ATP release from HK2 cells.

We used ATP biosensors to measure the real time release of ATP from HK2 cells treated for 48h +/- TGF-β1 (10ng/ml; Fig 8a). Biosensors recorded linear changes in ATP over a concentration of 0.1-100µM (Fig 8b/c and see [34]). In non-stimulated control cells the concentration of ATP released was 0.29 ± 0.06 µM (Fig 8d/f), which was significantly increased in TGF-β1 treated cells to 1.99 ± 0.47µM (Fig 8e/f, p<0.05, n=3).

Glucose evoked changes in ATP drive increased expression of inflammatory markers Interleukin 6 in HK2 cells

Recent studies have confirmed a link between renal connexin expression and tubule inflammation [21][37]. Elevated levels of nucleotides and altered connexin expression has been linked to inflammation and downstream fibrosis in multiple tissue types [38-44]. Having confirmed that glucose evoked changes in TGF-β1 drive increased expression of both CX26 and CX43, changes accompanied by increased hemichannel mediated ATP release, immunoblot analysis was used to assess the implications of TGF-β1 and ATP as downstream mediators of a glucose-evoked response on expression of inflammatory and fibrotic markers Interluekin-6 (IL-6) and fibronectin respectively.

HK2 cells were cultured in 5mM glucose for 48h prior to being serum starved overnight and then incubated for either 48h or 7days in TGF- β1 (2-10ng/ml). Immunoblot analysis confirmed that at 48h incubation with TGF- β1 (2-10 ng/ml), IL-6 expression was increased to 137.7±13.9%, 244.9±33.4% and 286.3±26.0% as compared to control (Fig9a p<0.001, n=4). Fibronectin expression increased to 129.5±11.7%, 176.4±30.4%, and 210±22.7% at 2, 4 and 10ng/ml compared to control respectively (Fig9b; p<0.001, n=4). At 7days incubation, IL-6 expression was increased to 690±88.9% as compared to control (Fig9c; p<0.05, n=3). Similarly, fibronectin expression increased to 188±12.8%, at 10ng/ml TGF- β1 as compared to control (Fig9d; p<0.05, n=3). These data confirm that TGF- β1 evokes increased expression of IL-6 and fibronectin in HK2 cells at both acute and chronic time periods.

To delineate a downstream role for ATP in mediating these-glucose evoked changes, HK2 cells were in the first instance incubated with non-hydroylsable ATPγS (1-100μM) for 48h. Expression of IL-6 (Fig10a) and fibronectin (Fig10b) was assessed by immunoblotting. ATPγS (1-100μM) evoked a significant increase in expression of IL-6 expression to 204.8±32.1%, 206.0±26.3% and 227.3±14.8% at 1, 10 and 100 μM compared to control respectively (Fig10a; $p<0.001$, n=4) and of fibronectin expression to 274.5±47.2%, 350.4±23.1% and 433.0±81.1% at 1, 10 and 100 μM as compared to control respectively (Fig10b; $p<0.001$, n=4).

Lastly, the link between TGF-β1 induced changes in ATP and altered expression of IL6 and fibronectin, was ascertained by incubating HK2 cells for 48hrs in TGF-β1 (10 ng/mL) +/-ATP diphosphohydrolase; apyrase (5 Units/ml). As expected TGF-β1 evoked an increase in both IL-6 and fibronectin to 274.1±35.5% (Fig10c), and 201.50±3.7% (Fig10d) respectively as compared to control ($p<0.01$ n=3). These changes were negated in part in the presence of apyrase, with expression reduced to 181.6±6.3%, and 156.7±27.6% for IL-6 and fibronectin respectively. Incubation of apyrase alone failed to exert any significant effect on expression.

To further delineate a role for ATP in mediating glucose-evoked changes at chronic intervals, HK2 cells were incubated with ATPγS (1-100 μM) for 7 days. Expression of IL-6 (Fig11a) and fibronectin (Fig11b) was assessed by immunoblotting. ATPγS(1-100 μM) evoked a significant increase in expression of IL-6 expression to 174.0±8.4%, 233.9±11.3% and 260.0±10.8% at 1, 10 and 100 μM compared to control respectively (Fig11a; $p<0.001$, n=4). Fibronectin expression also increased to 305.4±22.61%, 358.6±17.7% and 417.3±25.69% at 1, 10 and 100 μM as compared to control respectively (Fig11b; $p<0.001$, n=4). As with 48hrs, HK2 cells were also incubated for 7 days in TGF-β1 (10 ng/mL) +/- the ATP diphosphohydrolase; apyrase (5 Units/ml). As before, TGF-β1 evoked an increase in both IL-6 and fibronectin to 431.5±34.49% (Fig11c), and 262.4±42.5% (Fig11d) respectively as compared to control ($p<0.05$ n=3). These changes were negated in part in the presence of apyrase, with expression reduced to 190.9±47.92%, and 105.8±28.02% for IL-6 and fibronectin respectively. Incubation of apyrase alone failed to alter protein expression.

Discussion

Diabetes is the single commonest cause of entry into the renal replacement therapy programme and accounts for half of patients presenting with end-stage renal disease (ESRD) [1]. Approximately 21% of deaths in type1 diabetes and 11% of deaths in type2 diabetes are attributable to loss of renal function associated with diabetic nephropathy [43], a multifaceted complication which encompasses structural and functional disturbances including glomerular hyper-filtration, mesangial expansion, and interstitial fibrosis [2]. As a major underlying pathology of diabetic nephropathy, tubulointerstitial fibrosis develops under sustained hyperglycaemia, when early injury activates secretion of inflammatory mediators, infiltration of inflammatory cells, increased fibrotic deposition and overall loss of cell structure, function and integrity. [3]. Whilst current treatments focus on regulation of blood glucose and blood pressure [44], the ability to correct tubular inflammation and subsequent downstream fibrosis represents an unmet clinical need.

In diabetic nephropathy, the progression of tubular injury is associated with a number of morphological and phenotypic events [35][36]. Pivotal to these is the early loss of the adhesion protein epithelial (E)-cadherin, which forms part of the multi-protein adherens junction, linking cell-cell contact to the actin cytoskeleton and various signaling molecules [47]. Co-localized with E-cadherin at the sites of cell-cell contact [48], connexins oligomerise into hexameric hemi-channels/connexons that can form gap-junctions connecting the cytoplasm of adjoining cells [reviewed in 49]. Intercellular adhesion is a pre-requisite for gap junction formation. In the absence of neighboring binding partners, uncoupled hemi-channels permit local paracrine release of adenosine triphosphate (ATP) [4][6]. We previously reported that acute glucose evoked loss of cadherin mediated cell-cell coupling affected direct dye transfer between epithelial cells of the human proximal tubule [36]. The implications of this impaired adhesion and loss of dye transfer remain unresolved.

The present study correlates altered connexin expression to altered cell function in proximal tubular epithelial cells of the diabetic kidney. Novel histological evidence, suggests that expression of both CX26 and CX43 are significantly upregulated in tubules from renal biopsy material isolated from patients with diabetic nephropathy. These findings are further supported by observations that CX26 and CX43 exhibit increased expression in both our cell model and human primary proximal tubule cells at 7days incubation with TGF-β1. Interestingly, in the present study, the effect of TGF-β1 on connexin expression appears temporally dependent. Acute 48h incubation with glucose/TGF-β1 significantly reduced Smad2/3-dependent CX26 and CX43 expression in HK2 cells. However, chronic incubation with the same stimuli for 7days increased CX26 and CX43, a trend consistent with data from renal biopsy material isolated from patients with DN and with recent

16

reports that CXs appear to be upregulated in chronic kidney disease [20-21][49]. To delineate the functional consequences of this biphasic response, we used paired whole cell patch clamp recordings to directly measure how TGF-β1 affected GJIC. At both 48h and 7day incubation with the cytokine, junctional conductance was significantly reduced as compared to control. This counterintuitive finding can be explained by considering the relationship between cell-cell coupling and the ability of connexons to align and form functional gap-junctions [4-5][50]. Following acute challenge with high glucose and TGF-β1, connexin expression decreases providing less protein to form connexins and ultimately gap junctions. As expected, GJIC decreased. Contrary to this, chronic 7day incubation in high glucose/TGF-β1 increased the expression of both CX26 and CX43. This shift in expression should mean that there is more protein to form connexons and thus gap-junctions, however, junctional conductance was again reduced. This finding can be explained by drawing on our previous work, which suggests that glucose-evoked changes in TGF-β1 drives a loss of cell-to-cell adhesion [36]. With impaired cell-cell adhesion, connexons are unable to dock with similar hexameric units on adjacent cells and gap junctions fail to form [4-5]. In the absence of suitable binding partners, connexons exist as stand-alone pores. These hemi-channels are known to release nucleotides, in particular, ATP, as well as other small molecules and ions [6]. Under normal circumstances small amounts of ATP released into the microenvironment may provide a paracrine mechanism to maintain cell-to-cell communication. However, in chronic high glucose/TGF-β1, as associated with diabetes, up-regulation of connexin-mediated hemi-channels may overload this local diffusible route of communication. Several studies have suggested that there is a strict relationship between hemi-channel release of ATP and activation of purinergic receptors on neighbouring cells and that this may play a role in mediating the underlying pathology of various disease states [42][51-53]. Having confirmed that in both acute and chronic time points, glucose/TGF-β1 evoked changes in CX expression are paralleled by reduced GJIC, we wanted to determine if hemi-channel activity increased as a compensatory mechanism to maintain cell-to-cell communication. Carboxyfluorescein is a membrane impermeant dye that has been previously used to assess hemi-channel opening in a variety of cell types [31]. An increase in carbenoxleone-sensitive dye uptake suggested that the number and/or activity of hemi-channels was elevated in cells cultured in TGF-β1 for 48h and 7days. To confirm that the increase in channel opening correlated to a change in purinergic signalling, we used biosensors and demonstrated that increased hemichannel activity in TGF-β1 treated cells was matched by a significant increase in ATP release.

Recent studies confirm a link between hemi-channel mediated ATP release and progression and development of inflammation and fibrosis in multiple tissue types [38-41], including the diabetic kidney [42]. The connexin isoforms CX37 and CX40 have been highlighted as anti-inflammatory, whilst CX43 has been linked to inflammation [21]. Studies in the CX43 +/- mouse demonstrate reduced monocyte infiltration and reduced interstitial fibrosis, whilst administration of either a CX43

antisense or inhibition of CX43 with the Gap26 mimetic peptide, partly negate the inflammatory and fibrotic changes as seen in the interstitium of a mouse model of CKD [21]. Preclinical studies addressing a role for ATP in the pathology of diabetic nephropathy are somewhat limited, perhaps reflecting a lack of suitable mouse models of this disease. Nevertheless, activation of the NLRP3 inflamasome and subsequent activation of proinflammatory markers interleukin 1 beta (IL-1β) and interleukin 18 (IL18) have been linked to elevated extracellular ATP levels and enhanced purinergic signaling [54-58]. Once in the extracellular environment, these interleukins produce an array of inflammatory proteins including TNF-α and IL-6 that are instrumental in the pathology of tubular inflammation and fibrosis [59-60]. Associated with abberant increased synthesis of the extracellular matrix (ECM) remodelling, ATP has also been suggested to be play a key role in ECM remodelling and subsequent fibrosis [55]. Studies by Solini et al confirmed that exogenous application of ATP to rat mesangial cells, triggered a concentration dependent increase in the ECM markers, fibronectin, collagen IV, laminin and pro-fibrotic TGF-β [55]. These changes were negated by pre-incubation of high glucose with apyrase, a calcium-activated membrane-bound enzyme that catalyses the hydrolysis of ATP to AMP and inorganic phosphate, thereby deactivating ATP [55]. In the current study, our novel data suggests, that cells shift from GJIC to hemi-channel mediated ATP release as they attempt to maintain cell-to-cell communication and overall function. Interestingly, with increased hemi-channel mediated ATP release having been linked to fibrosis in multiple disease states [38-39], it is likely that this mechanism may contribute to tubular injury through increased ATP-driven fibrosis. Certainly our data would suggest that in an attempt to maintain epithelial cell-to-cell communication in late stage nephropathy, imbalance in connexin expression/function could actually exacerbate disease progression, with increased hemichannel mediated ATP release driving increased expression of proinflammatory IL-6 and profibrotic fibronectin. Whilst our understanding of the complex interplay between connexins, nucleotide release and downstream purinergic signalling in hyperglycaemia remains rudimentary, it is clear that connexins offer a viable future target in the therapeutic control and treatment of this chronic debilitating metabolic condition and command further future investigation.

Figure legends

Fig. 1: CX26 and CX43 expression is upregulated in biopsy material isolated from patients with proven nephropathy. Immunohistochemical staining of CX26 (Fig 1a) and CX43 (Fig 1c) in human renal tissue from patients with biopsy proven diabetic nephropathy is shown in panels A and B and for non-diabetic control subjects in panels C and D. Isotype-matched negative control (Fig 1e is shown in non-diabetic controls (Panel A) and diabetic nephropathy (panel B). Magnification: 400X. Quantitative analysis of CX26 (Fig 1b) and CX43 (Fig 1d) staining was performed by Image Pro Plus 6.0 software; IOD, Integrated Optical Density. **$P<0.01$ compared with control.

Fig. 2: Glucose-evoked increases in TGF-β1 stimulate morphological changes associated with early tubular injury. HK2 cells were cultured in low glucose (5mmol/l), high glucose (25mmol/l) or an osmotic control (OC, L-glucose; 25mmol/L). The supernatant was removed and TGF-β1 secretion quantified by ELISA (Fig 2a). Secreted TGF-β1 was activated by a repeat freeze-thaw procedure of conditioned media. Phase contrast microscopy (Fig 2b) and TRITC conjugated phalloidin (Fig 2c) assessed cell morphology and cytoskeletal organization respectively in low glucose (5mmol/l), conditioned media (25mmol/l), TGF-β1 (10ng/ml) and high glucose (25mmol/l) for 48h.

Fig. 3: Glucose and TGF-β1 evoke a loss in CX26 and CX43 expression at 48h. HK2 cells were cultured in low glucose (5mmol/l, control), conditioned medium (25mmol/l CM), L-glucose (OC, 25mmol/l) and high glucose (25mmol/l) (panels a and b) or in low glucose (5mmol/l) with or without TGF-β1 (2-10ng/ml) for 48h (panels c and d). Whole-cell abundance of CX26 (Fig 3a & 3c) and CX43 (Fig 3b and 3d) were determined by immunoblotting. Representative blots are shown for each protein with re-probing for α-tubulin as loading control. Semi-quantification (mean ± SEM) was by densitometry, normalized against the non-stimulated low glucose control (100%). Bars correspond to associated lanes in the respective blot. Results were from three or more separate experiments; *$P<0.05$, **$P<0.01$ and ***$P<0.001$.

Fig. 4: TGF-β1 evokes an increase in CX26 and CX43 expression at 7days incubation. HK2 (Fig 4b and 4c) and hPTEC cells (Fig 4a, d and e) were cultured with or without TGF-β1 (10ng/ml) for 7days. Phase contrast morphology of control hPTEC (panel A) and TGF-β1 (10ng/ml) (panel B) treated hPTECs at 7days is shown in Fig 4a

Whole-cell abundance of CX26 (Fig 4b & 4d) and CX43 (Fig 4c and 4e) were determined by immunoblotting in HK2 and hPTECs respectively. Representative blots are shown for each protein with re-probing for α-tubulin as loading control. Semi-quantification (mean ± SEM) was by densitometry, normalized against the non-stimulated low glucose control (100%). Bars correspond to associated lanes in the respective blot. Results were from three or more separate experiments; *$P<0.05$, **$P<0.01$ and ***$P<0.001$.

Fig. 5: TGF-β1 regulates CX26 and CX43 expression via SMAD2/3 signalling. TGF-β1 stimulates phosphorylation of SMAD2 (Fig 5a) and SMAD3 (Fig 5b) in HK2 cells. Knockdown of both SMAD2 at 48hrs and 96hrs respectively (Fig 5c & 5d) and SMAD3 at 48hrs and 96hrs respectively (Fig 5e & 5f) was achieved using siRNA. Representative blots show changes in protein for transfection reagent (TR) alone, SMAD siRNA (S2 and S3) and scrambled siRNA (SS) versus the same blot stripped and re-probed for α-tubulin as a loading control. HK2 cells were then transfected for 48h with either SMAD2 or SMAD3 siRNA. Post transfection, cells were stimulated with TGF-β1 (10ng/ml) for 48h and expression of CX26 and CX43 assessed. Whole cell protein expression of CX26 (Fig 5g) and CX43 (Fig. 5h) were determined by immunoblotting. Representative blots are shown for each protein with re-probing for α-tubulin. Semi-quantification (mean ± SEM) was by densitometry, normalized against non-stimulated low glucose control (100%). Bars correspond to the associated lanes in the respective blot. Results were from three or more separate experiments; ***$P<0.001$.

Fig. 6: TGF-β reduces junctional conductance between coupled HK2 cells. Panel a, Paired whole cell patch clamp recordings from coupled cells in control, cells treated with TGF-β1 (10 ng/ml) for 48 hours and cells treated with TGF-β1 (10 ng/ml) for 7 days. Hyperpolarizing and depolarizing current steps (20 pA, -40 to 40 pA) injected into cell-1 produced voltage responses in cell-2 demonstrating electrical coupling. The inset is a micrograph showing electrode positions during a recording from coupled cells. Panel b, Graph plotting the mean junctional conductance for pairs of cells in control versus cells treated with TGF-β1 (10 ng/ml) for 48h and 7days. The junctional conductance is significantly reduced in TGF-β1 treated cells at 48 h (1.15±0.9nS) and 7 days (0.42±0.2nS) compared to control (4.5±1.3nS; * $P<0.05$).

Fig. 7: TGF-β1 increases hemi-channel dependent dye loading in HK2 cells.
Carboxyfluorescein (200μM) loading in 48h (Fig 7a and b) and 7day (Fig 7c and d) control and TGF-β1 (10ng/ml) treated HK2 cells with and without carbenoxolone (CBX; 200μM). Minimal dye loading is visible in control cells at 48h (Fig 7a) and 7days (Fig 7c). There is strong dye loading in cells cultured with TGF-β1 at both time points, consistent with an increased number/opening of connexin hemi-channels. Addition of carbenoxolone (200μM) significantly reduced the dye loading. Pixel intensity from TGF-β1 treated cells expressed as a percentage of control at 48h (Fig 7b) and 7days (Fig. 7d) demonstrates that opening of the hemi-channels by removal of extracellular calcium (10 min) significantly increases dye uptake at 48 h (378 ± 33%) or 7days (430 ±18%). Addition of carbenoxolone (200μM) prevented cytokine-evoked changes at both time intervals (110±5.4% of control at 48h and 64±2.6% of control at 7days). Pixel intensity was recorded for 10 cells in 3 separate experiments; $**P<0.01$ and $***P<0.001$.

Fig. 8: TGF-β1 increases hemi-channel mediated ATP release. Fig 8a, shows the experimental recording configuration with both ATP and null sensors (2 mm sensing area) situated horizontally above the HK2 cells. Fig 8b, ATP biosensor trace showing responses to different concentrations of ATP. Inset, Graph plotting current against ATP concentration (Fig 8c). ATP biosensors show a linear response to increasing concentrations of ATP (n = 3 for each point). No changes in baseline current were observed on null sensors (data not shown). (Fig 8d and 8e) Representative ATP biosensor traces showing the effect of calcium removal following 48h treatment with either control (Fig. 8d) or TGF-β1 (10ng/ml; Fig 8e). Cells cultured in TGF-β1 exhibit a discernable release of ATP when extracellular calcium is removed whereas there is little or no response in control cells. Application of 10 μM ATP at the end of the experiment is used for calibration and shows that the biosensor sensitivity was similar for both treatments. Fig 8f, graph plotting the mean data demonstrating the effect of TGF-β1 versus control on the amount ATP release following 48h incubation. Cells cultured with the cytokine exhibited a 7fold increase in ATP release compared to control (1.99 ± 0.47 μM versus 0.29 ± 0.06 μM; $P<0.05$).

Fig. 9: TGF-β1 upregulates expression of Interleukin-6 and Fibronectin at 48h and 7 days.
HK2 cells were initially cultured in TGF-β1 (2-10ng/ml) for 48h, ahead of chronic incubation at 7days in TGF-β1 (10ng/ml). Whole-cell expression of pro-inflammatory IL-6 and pro-fibrotic fibronectin were determined by immunoblotting at 48h TGF-β1 incubation (Fig 9a and 9b respectively). For chronic treatment, cells were cultured in low glucose (5mmol/l) with or without TGF-β1 (10ng/ml) for 7days and whole-cell expression of IL-6 and fibronectin assessed (Fig 9c and 9d respectively). Representative blots are shown for each protein with re-probing for α-tubulin as loading control. Semi-quantification (mean ± SEM) was by densitometry, normalized against the non-stimulated low glucose control (100%). Bars correspond to associated lanes in the respective blot. Results were from three or more separate experiments; $*P<0.05$, $**P<0.01$ and $***P<0.001$.

Fig. 10: ATP drives increased expression Interleukin-6 and Fibronectin at 48hrs and 7 days.
Glucose evoked changes in TGF-β1 drive altered IL6 and fibronectin expression through downstream ATP signaling. HK2 cells were cultured in low glucose (5mmol/l, control) with or without ATPγS (1-100μM/ml) for 48h. Whole-cell expression of IL-6 (Fig 10a) and fibronectin (Fig. 10b) were determined by immunoblotting. Confirmation of a role for ATP in mediating the TGF-β1 induced response as observed in Fig 9; was determined by incubating cells with TGF-β1 with or without Apyrase for 48h. Whole-cell expression of IL-6 (Fig 10c) and fibronectin (Fig 10d) were determined by immunoblotting. Representative blots are shown for each protein with re-probing for α-tubulin as loading control. Semi-quantification (mean ± SEM) was by densitometry, normalized against the non-stimulated low glucose control (100%). Bars correspond to associated lanes in the respective blot. Results were from three or more separate experiments; $*P<0.05$, $**P<0.01$ and $**P<0.01$.

Fig. 11: ATP drives increased expression Interleukin-6 and Fibronectin at 7 days.
HK2 cells were cultured in low glucose (5mmol/l, control) with or without ATPγS(1-100μM/ml) for 7 days. Whole-cell expression of IL-6 (Fig 11a) and fibronectin (Fig. 11b) were determined by immunoblotting. To establish a role for ATP in mediating TGF-β1 induced response as observed in Fig 9; HK2 cells were incubated with TGF-β1 with or without Apyrase for 7 days and whole-cell expression of IL-6 (Fig 11c) and fibronectin (Fig 11d) assessed. Representative blots are shown for each protein with re-probing for α-tubulin as loading control. Semi-quantification (mean ± SEM) was by densitometry, normalized against the non-stimulated low glucose control (100%). Bars correspond to associated lanes in the respective blot. Results were from three or more separate experiments; $*P<0.05$, $**P<0.01$ and $***P<0.01$.

Competing Interests

The authors declare that they have no competing interests.

Contribution statement:

CEH & PES conceived the study design and were involve in the research planning of the project. CEH orchestrated and supervised all experimental outcomes with GWP. SWT and WY performed immunohistochemistry on human biopsy samples, whilst MJW and TJK contributed to electrophysiology and bio-sensing. All authors contributed to the intellectual content of the article.

References:

1. http://www.diabetes.org.uk

2. Zeisberg M, Neilson EG: Mechanisms of Tubulointerstitial Fibrosis. JASN 2003;21:1819-1834.

3. Wada J, Makino H: Inflammation and the pathogenesis of diabetic nephropathy. Clin Sci 2013; 124:139-152.

4. Vinken M: Introduction: connexins, pannexins and their channels as gatekeepers of organ physiology. Cell Mol Life Sci 2015;72:2775-2778.

5. Bosco D, Haefliger JA, Meda P: Connexins: key mediators of endocrine function. Physiol Rev 2011;91:1393-1445.

6. Wang N, De Bock M, Decrock E, Bol M, Gadicherla A, Vinken M, Rogiers V, Bukauskas FF, Bultynck G, Leybaert L: Paracrine signaling through plasma membrane hemichannels. Biochimica et Biophysica Acta (BBA) - Biomembranes 2013;1828:35–50.

7. Morel S, Christoffersen C, Axelsen LN , Montecucco F, Rochemont V, Frias MA, Mach F, James RW, Naus CC, Chanson M, Lampe PD, Nielsen MS, Nielsen LB, Kwak BR: Sphingosine-1-phosphate reduces ischaemia-reperfusion injury by phosphorylating the gap junction protein Connexin43. Cardiovasc Res 2016;109:385-396.

8. Diezmos EF, Bertrand PP, Liu L: Purinergic Signaling in Gut Inflammation: The Role of Connexins and Pannexins. Front Neurosci 2016;10:311.

9. Le Gal L, Alonso F, Mazzolai L, Meda P, Haefliger J-A: Interplay between connexin40 and nitric oxide signaling during hypertension. Hypertension 2015; 65:910-915.

10. Wang L-J, Liu W-D, Zhang L, Ma K-T, Zhao L, Shi W-Y, Zhang WW, Wang YZ, Li L, Si JQ: Enhanced expression of Cx43 and gap junction communication in vascular smooth muscle cells of spontaneously hypertensive rats. Mol Med Rep 2016;14:4083-4090.

11. Li H, Wang F: The role of connexin43 in diabetic microvascular complications, Discov Med 2016;22:275-280.

12. Kuczma M, Wang CY, Ignatowicz L, Gourdie R, Kraj P: Altered connexin 43 expression underlies age-dependent decrease of regulatory T cell suppressor function in non-obese diabetic mice. J Immunol 2015;194:5261-5271.

13. Xie X, Lan T, Chang X, Huang K, Huang J, Wang S, Chen C, Shen X, Liu P, Huang H: Connexin43 mediates NF-κB signalling activation induced by high glucose in GMCs: involvement of c-Src. Cell Commun Signal 2013;11:38.

14. Roy S, Kern TS, Song B, Stuebe C: Mechanistic Insights into Pathological Changes in the Diabetic Retina: Implications for Targeting Diabetic Retinopathy. Am J Pathol 2017;187:9–19.

15. Wright JA, Richards T, Becker DL: Connexins and diabetes. Cardiol Res Pract 2012;2012:496904.

16. Wang CM, Lincoln J, Cook JE, Becker DL: Abnormal connexin expression underlies delayed wound healing in diabetic skin. Diabetes 2007;56:2809-2817.

17. Bobbie MW, Roy S, Trudeau K Munger SJ, Simon AM, Roy S: Reduced connexin 43 expression and its effect on the development of vascular lesions in retinas of diabetic mice. Invest Ophthalmol Vis Sci 2010;51:3758-3763.

18. Moore K, Ghatnekar G, Gourdie RG, Potts JD: Impact of the controlled release of a connexin 43 peptide on corneal wound closure in an STZ model of type I diabetes. PLoS One 2014;23:9.

19. Tien T, Muto T, Barrette K, Challyandra L, Roy S: Downregulation of Connexin 43 promotes vascular cell loss and excess permeability associated with the development of vascular lesions in the diabetic retina. Mol Vis 2014;2:732-741.

20. Toubas J, Beck S, Pageaud A-L, Huby A-C, Mael-Ainin M, Dussaule J-C, Chatziantoniou C, Chadjichristos CE: Alteration of connexin expression is an early signal for chronic kidney disease. Am J Physiol Renal Physiol 2011;301:F24–32.

21. Abed A, Toubas J, Kavvadas P, Authier F, Cathelin D, Alfieri C, Boffa JJ, Dussaule JC, Chatziantoniou C, Chadjichristos CE: Targeting connexin 43 protects against the progression of experimental chronic kidney disease in mice. Kidney Int 2014;86: 768–779.

22. Hu C, Cong XD, Dai DZ, Zhang Y, Zhang GL, Dai Y: The Renal Connexome and Possible Roles of Connexins in Kidney Diseases. Am J Kidney Dis 2016;67:677–687.

23. Hanner F, Sorensen C.M, Holstein-Rathlou N.H, Peti-Peterdi J: Connexins and the kidney. Am J Physiol Regul Integr Comp Physiol 2010;298:R1143–1155.

24. Loeffler I, Wolf G: Transforming growth factor-β and the progression of renal disease. Nephrol Dial Transplant 2014;29 Suppl 1:i37–i45.

25. Yiu WH, Wong DW, Chan LY, Leung JC, Chan KW, Lan HY, Lai KN, Tang SC: Tissue kallikrein mediates pro-inflammatory pathways and activation of protease-activated receptor-4 in proximal tubular epithelial cells. PLoS One 2014;9:e88894.

26. Siamantouras E, Hills CE, Squires PE, Liu KK: Quantifying cellular mechanics and adhesion in renal tubular injury using single cell force spectroscopy. Nanomedicine. 2016;12:1013-1021.

27. Fraser D, Brunskill N, Ito T, Phillips A. Long-term exposure of proximal tubular epithelial cells to glucose induces transforming growth factor-beta 1 synthesis via an autocrine PDGF loop. Am J Pathol. 2003;163:2565-2574.

28. Phillips AO, Steadman R, Morrisey K, Williams JD:
Polarity of stimulation and secretion of transforming growth factor-beta 1 by cultured proximal tubular cells. Am J Pathol 1997;150:1101-1111.

29. Hills CE, Bland R, Bennett J, Ronco PM, Squires PE: High glucose up-regulates ENaC and SGK1 expression in HCD-cells. Cell Physiol Biochem 2006;18:337-346.

30. Hills CE, Bland R, Wheelans DC, Bennett J, Ronco PM, Squires PE: Glucose-evoked alterations in connexin43-mediated cell-to-cell communication in human collecting duct: a possible role in diabetic nephropathy. Am J Physiol Renal Physiol 2006;291:F1045–1051.

31. Hills CE, Kerr MI, Wall MJ, Squires PE: Visfatin reduces gap junction mediated cell-to-cell communication in proximal tubule-derived epithelial cells. Cell Physiol Biochem 2013;32:1200-1212.

32. Llaudet E, Botting NP, Crayston JA, Dale N: A three-enzyme microelectrode sensor for detecting purine release from central nervous system. Biosensors and Bioelectronics 2003;18:43-52.

33. Llaudet E, Hatz S, Droniou M, Dale N: Microelectrode Biosensor for Real-Time Measurement of ATP in Biological Tissue. Anal Chem 2005;77:3267–3273.

34. Huckstepp RTR, Eason R, Sachdev A, Dale N: CO2-dependent opening of connexin 26 and related β connexins. J Physiol 2010;588:3921–3931.

35. Hills CE, Squires PE: The role of TGF-β and epithelial-to mesenchymal transition in diabetic nephropathy. Cytokine Growth Factor Rev 2011;22:131-139.

36. Hills CE, Siamantouras E, Smith SW, Cockwell P, Liu KK, Squires PE: TGFβ modulates cell-to-cell communication in early epithelial-to-mesenchymal transition. Diabetologia 2012;55:812-824.

37. Abed A, Dussaule J-C, Boffa J-J, Chatziantoniou C, Chadjichristos CE: Connexins in renal endothelial function and dysfunction. Cardiovasc Hematol Disord Drug Targets 2014;14:15–21.

38. Lu D, Soleymani S, Madakshire R, Insel PA: ATP released from cardiac fibroblasts via connexin hemichannels activates profibrotic P2Y2 receptor. FASEB 2012;26:2580–2591.

39. Riteau N, Gasse P, Fauconnier L, Gombault A, Couegnat M, Fick L, Kanellopoulos J, Quesniaux VF, Marchand-Adam S, Crestani B, Ryffel B: Extracellular ATP Is a Danger Signal Activating P2X7 Receptor in Lung Inflammation and Fibrosis. Am J Respir Crit Care Med 2010;182:774–783.

40. Tung HC, Lee FY, Wang SS, Tsai MH, Lee JY, Huo TI, Huang HC, Chuang CL, Lin HC, Lee SD: The Beneficial Effects of P2X7 Antagonism in Rats with Bile Duct Ligation-induced Cirrhosis. PloS One 2015;1:e0124654.

41. Ferrari D, Gambari R, Idzko M, Müller T, Albanesi C, Pastore S, La Manna G, Robson SC, Cronstein B: Purinergic signaling in scarring. FASEB J 2016;30:3–12.

42. Solini A, Usuelli V, Fiorina P: The Dark Side of Extracellular ATP in Kidney Diseases. J Am Soc Nephrol 2015;26:1007–1016.

43. Solini A, Menini S, Rossi C, Ricci C, Santini E, Blasetti Fantauzzi C, Iacobini C, Pugliese G: The purinergic 2X7 receptor participates in renal inflammation and injury induced by high-fat diet: possible role of NLRP3 inflammasome activation. J Pathol 2013;231:342–353.

44. Menzies RI, Tam FW, Unwin RJ, Bailey MA: Purinergic signaling in kidney disease. Kidney Int 2017;91:315-323.

45. http://www.cdc.gov/diabetes/statistics/complications_national.htm

46. Xue R, Gui D, Zheng L, Zhai R, Wang F, Wang N: Mechanistic Insight and Management of Diabetic Nephropathy: Recent Progress and Future Perspective. J Diabetes Res 2017;2017:1839809.

47. Siamantouras E, Hills CE, Squires PE, Liu KK: Quantifying cellular mechanics and adhesion in renal tubular injury using single cell force spectroscopy. Nanomedicine 2016;12:1013-1021.

48. Meng W, Takeichi M: Adherens junction: molecular architecture and regulation, Cold Spring Harb Perspect Biol 2009;1:a002899.

49. Fujimoto K, Nagafuchi A, Tsukita S, Kuraoka A, Ohokuma A, Shibata Y: Dynamics of connexins, E-cadherin and alpha-catenin on cell membranes during gap junction formation. J Cell Sci 1997; 110:311-322.

50. Esseltine JL, Laird DW: Next-Generation Connexin and Pannexin Cell Biology, Trends Cell Biol. 2016;26:944-955.

51. Evans W, De Vuyst E, Leybaert L: The gap junction cellular internet: connexin hemichannels enter the signalling limelight, Biochem J 2006;1;39:1-14.

52. Sala G, Badalamenti S, Ponticelli C: The Renal Connexome and Possible Roles of Connexins in Kidney Diseases. Am J Kidney Dis 2016;67:677-687.

53. Hills CE, Price GW, Squires PE: Mind the gap: connexins and cell-cell communication in the diabetic kidney. Diabetologia 2015;58:233-241.

54. Gombault A, Baron L, Couillin I. ATP release and purinergic signaling in NLRP3 inflammasome activation. Front Immunol. 2012;3:414.

55. Solini A, Iacobini C, Ricci C, Chiozzi P, Amadio L, Pricci F, Di Mario U, Di Virgilio F, Pugliese G: Purinergic modulation of mesangial extracellular matrix production: Role in diabetic and other glomerular diseases. Kidney Int 2005;67:875–885.

56. Maes M, Crespo Yanguas S, Willebrords J, Cogliati B, Vinken M: Connexin and pannexin signaling in gastrointestinal and liver disease. Transl Res. 2015;166:332-343.

57. Chen K, Zhang J, Zhang W, Zhang J, Yang J, Li K, He Y: ATP-P2X4 signaling mediates NLRP3 inflammasome activation: A novel pathway of diabetic nephropathy. Int J Biochem Cell Biol. 2013;45:932-943.

58. Masood H, Che R, Zhang A: Inflammasomes in the Pathophysiology of Kidney Diseases. Kidney Dis 2015;1:187-193.

59. Anders HJ: Of Inflammasomes and Alarmins: IL-1β and IL-1α in Kidney Disease. J Am Soc Nephrol 2016;27:2564-2575.

60. Qiu YY, Tang LQ: Roles of the NLRP3 inflammasome in the pathogenesis of diabetic nephropathy, Pharmacol Res. 2016;114:251-264.

Figure 1:

a

TGF-β1 secretion pg/mL

1500

1000

500

0

***

5mM   25mM   OC

b

Control

Conditioned Media (25mM)

TGF-β1 (10ng/mL)

Glucose (25mM)

c

Control

Conditioned Media (25mM)

TGF-β1 (10ng/mL)

Glucose (25mM)

Figure 2:

Figure 3:

Figure 4:

a

pSMAD2
60kDa

SMAD2
60kDa

0 5 10 15 30 1 2 4 6

b

pSMAD3
53kDa

SMAD3
53kDa

0 5 10 15 30 1 2 4 6

c

Smad2
60kDa

α-tubulin
50kDa

***

SMAD2 Expression
(% as compared to control)

5mM TR S2 SS

d

Smad2
60kDa

α-tubulin
50kDa

***

SMAD2 Expression
(% as compared to control)

5mM TR S2 SS

e

Smad3
60kDa

α-tubulin
50kDa

***

SMAD3 Expression
(% as compared to control)

5mM TR S3 SS

f

Smad3
60kDa

α-tubulin
50kDa

***

SMAD3 Expression
(% as compared to control)

5mM TR S3 SS

g

CX26
26kDa

α-tubulin
50kDa

***
***
***

CX26 Expression
(% as compared to control)

5mM TGF-β1 S2 S3

h

CX43
43kDa

α-tubulin
50kDa

***
***
***

CX43 Expression
(% as compared to control)

5mM TGF-β1 S2 S3

Figure 5:

a

Control   TGF-β1 (2d)   TGF-β1 (7d)

cell 1   cell 1   cell 1

cell 2   cell 2   cell 2

10mV

100ms

b

Figure 6:

Figure 7:

a

b

Calibration

1µM   10µM   100µM   50µM   25µM

0.5mA

200secs

c

Current (mA)

[ATP] (µM)

d

Control

10µM

1mA

100secs

e

TGF-β1

10µM

1mA

100secs

f

[ATP] (µM)

*

0   10

TGF-β1 (ng/ml)
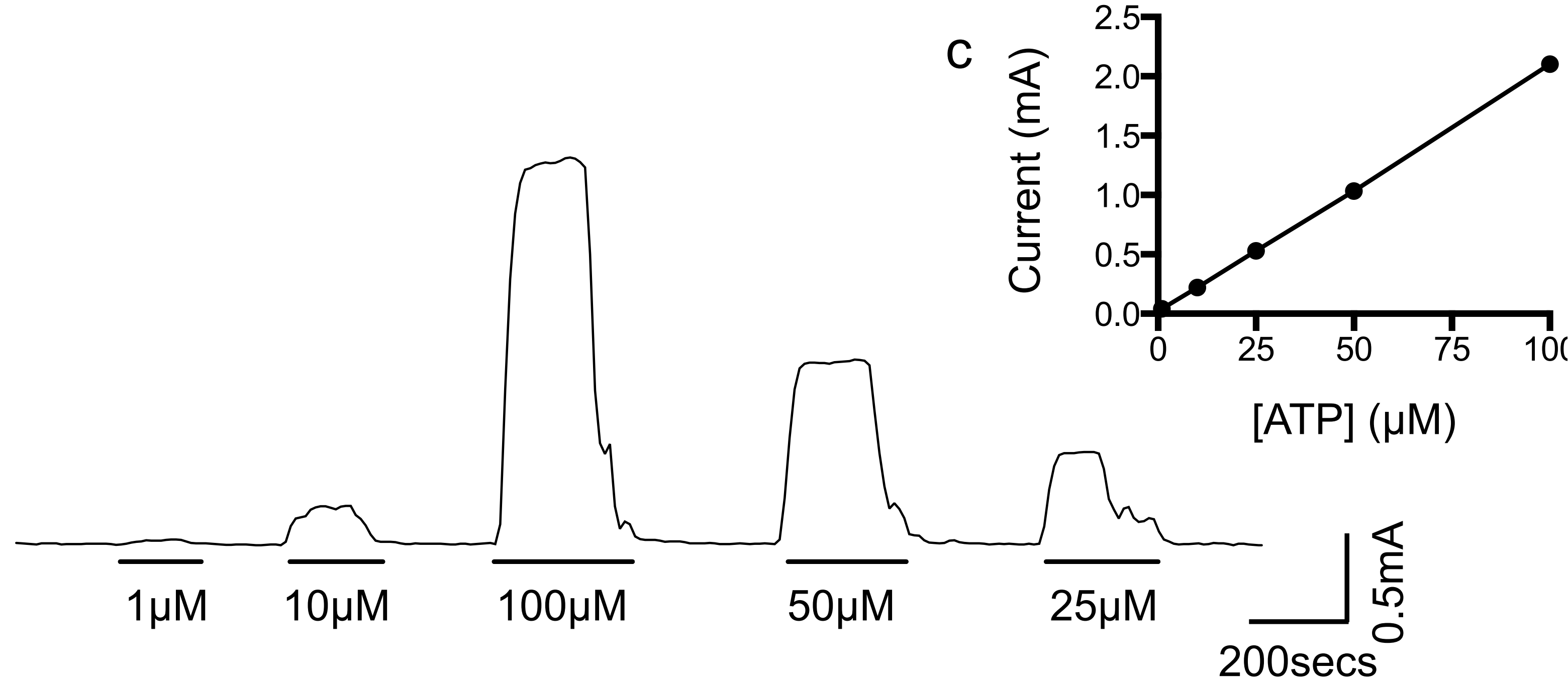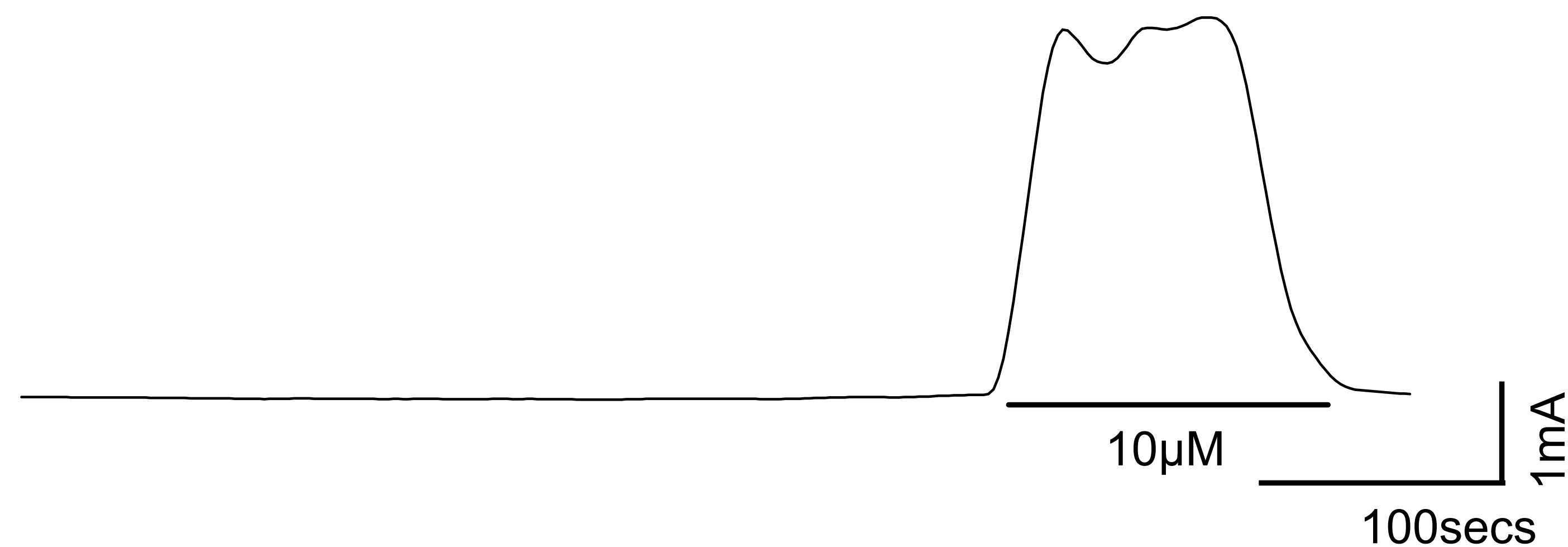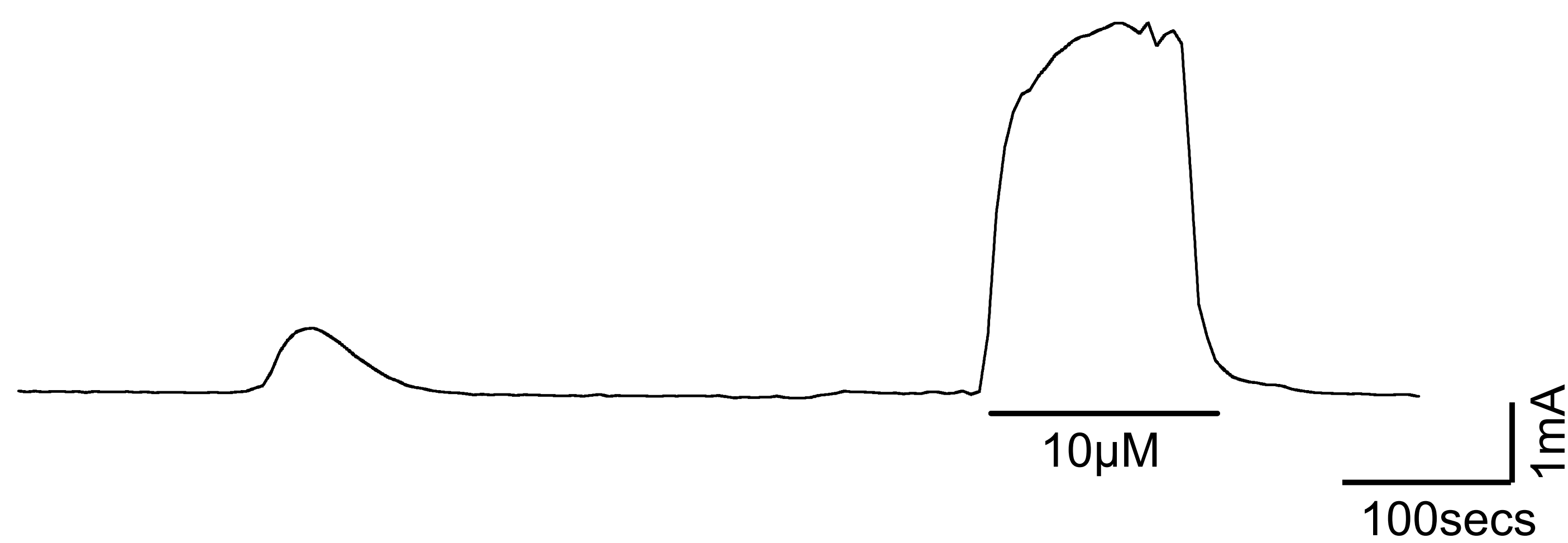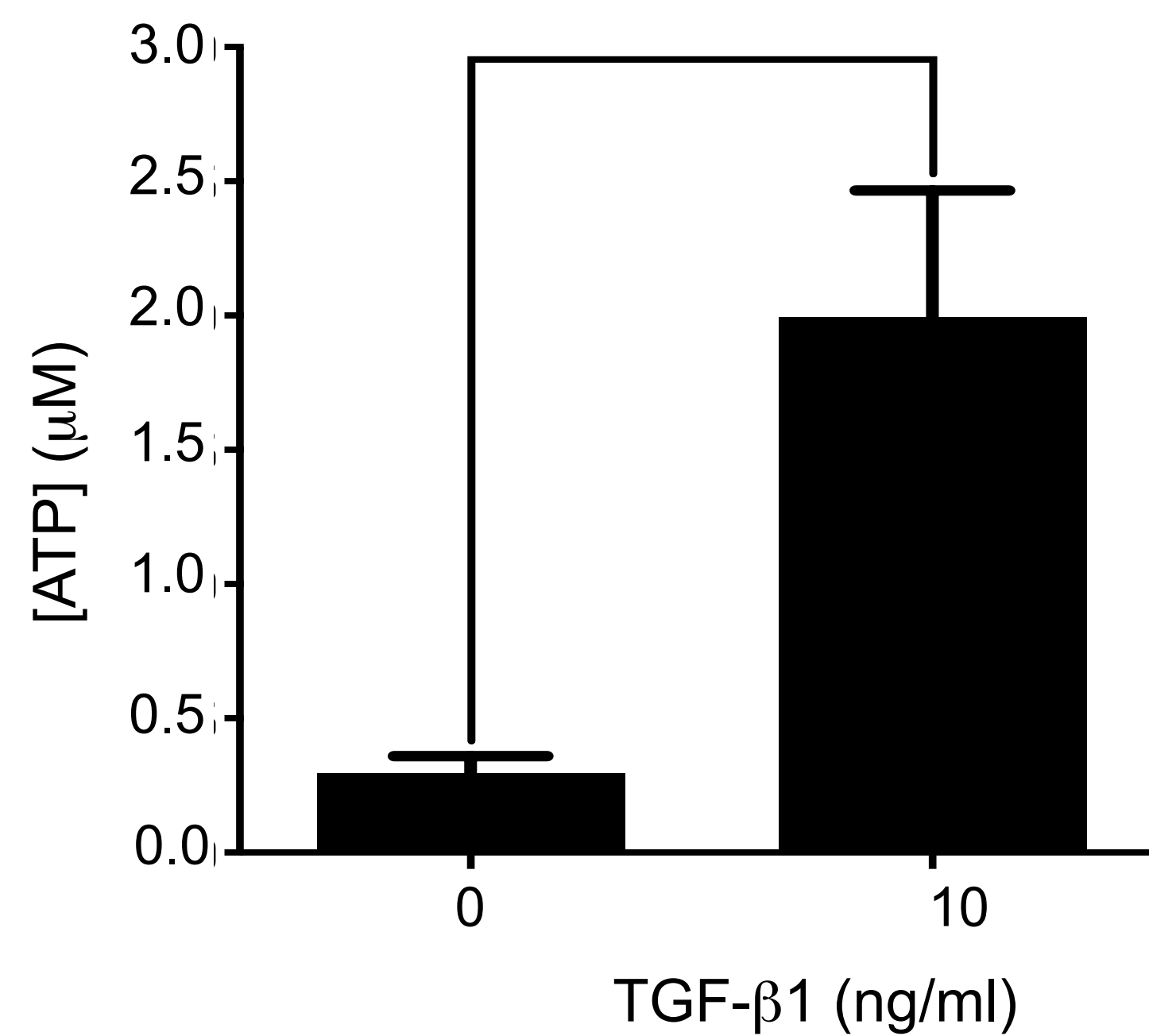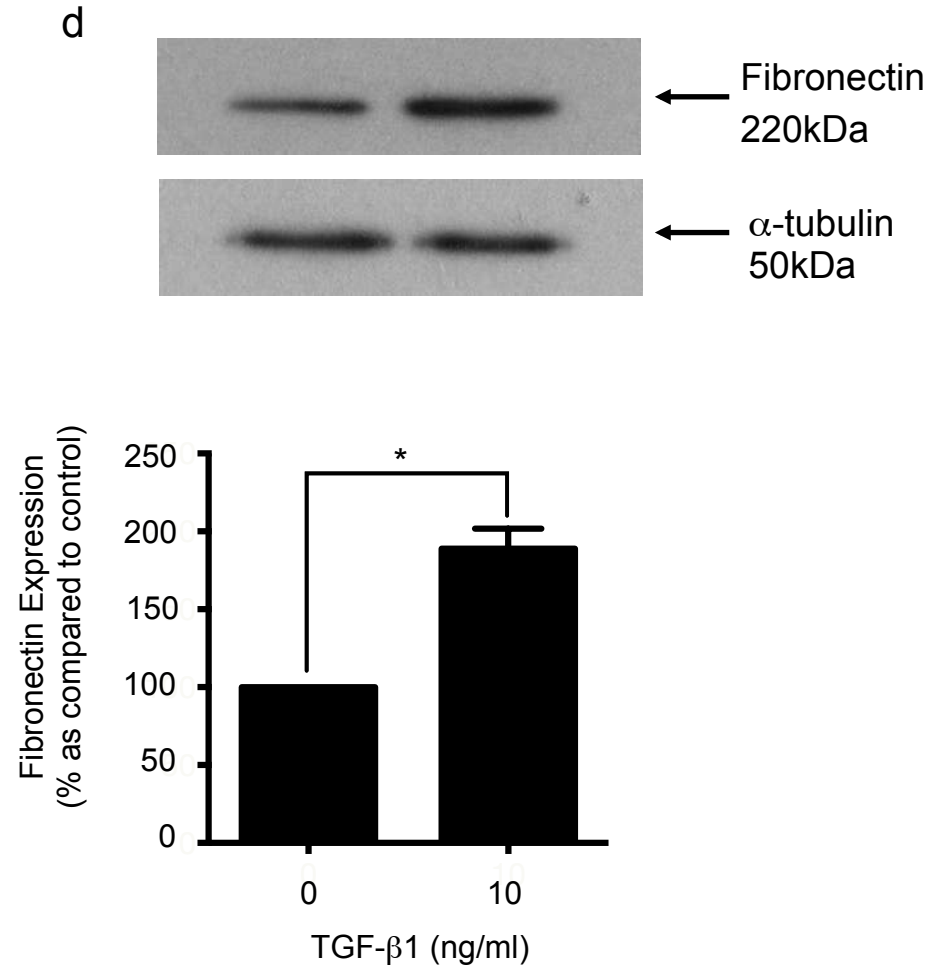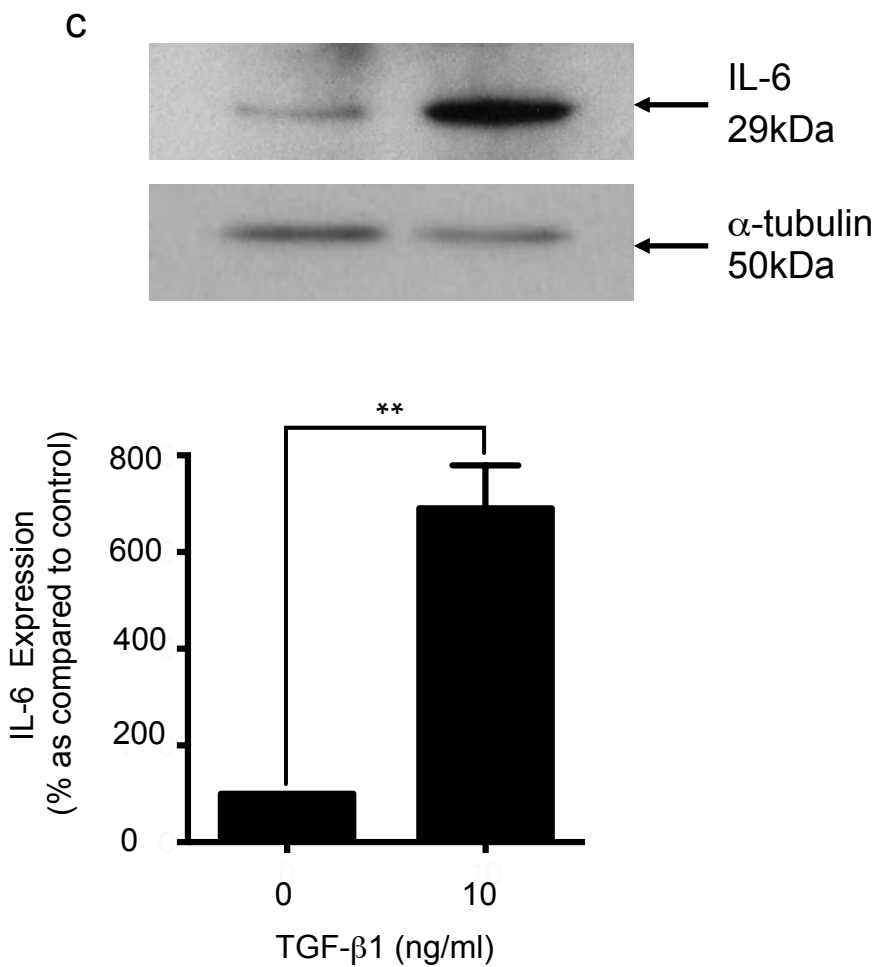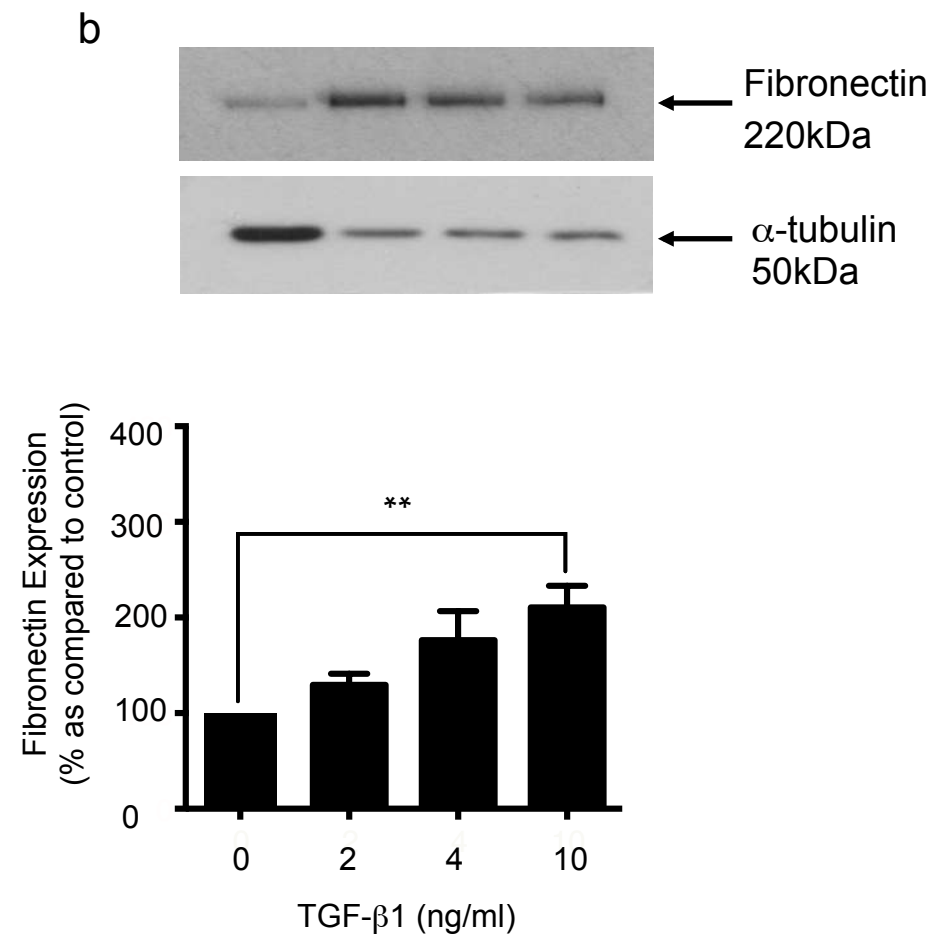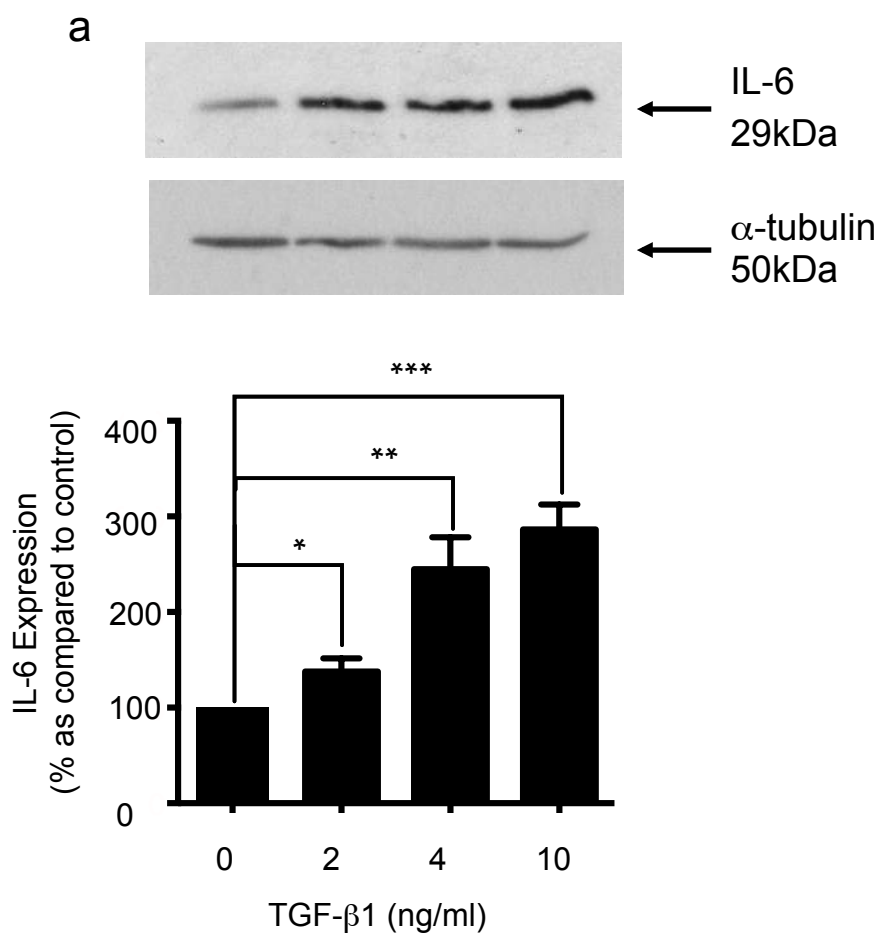
Figure 8:

Figure 9:

Figure 10:

Figure 11: